



Received: 23-04-2026  
Accepted: 03-06-2026

ISSN: 2583-049X

## Displacement of Water Molecules from Receptor-Ligand Interface During Binding Interaction

Ikechukwu Iloh Udema

Department of Chemistry and Biochemistry, Research Division, Ude International Concepts Ltd., 862217, B. B. Agbor, Delta State, Nigeria

Corresponding Author: Ikechukwu Iloh Udema

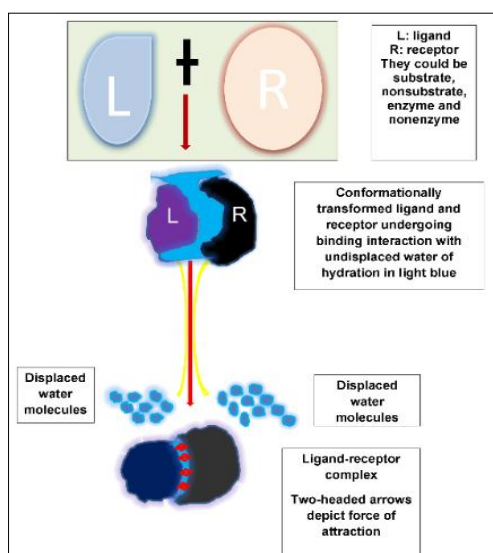
### Abstract

In almost all studies on the role of solvent in the binding of the ligand to a receptor, the focus had always been on the thermodynamic stability of the complex formed. Hardly any attempt has been made to quantify the number of solvent molecules released in the course of ligand (*e.g.*, substrate, pathogen, drug, *etc.*) and receptor (enzymes, cell membrane, antibodies, *etc.*) binding interaction in recent times. The goal of the study was to determine how to calculate the amount of solvent molecules displaced from reactant species using nonequilibrium binding energy (NEBE), since desolvation is a prerequisite for the development of a stable complex. Deriving relevant energy equations, such as the one for calculating the number of molecules of desolvation, was one of the objectives. The methods are solely theoretical, experimental (Bernfeld), and computational. According to the study's findings, the water of hydration ranged from 338

to 400 water molecules per molecule of complex, which corresponded to substrate (gelatinized potato starch) concentrations between 5 and 10 g/L. The translational entropy gains, the corresponding thermodynamic component, ranged from 93.06 to 136.70 *exp.* ( $-3$ ) J/mol K. The comparable values were 526.316 water molecules and 216.129 *exp.* ( $-3$ ) J/mol K, respectively, at the highest hydrolysis velocity. In conclusion, the equation of NEBE can be explored for the computation of water of desolvation in support of the observation that desolvation is part of the driving forces that propel ligand-receptor binding. Further thermodynamic characterization of ligand-receptor binding on the basis of desolvation needs to be done at different temperatures in the future. **PACS Number:** 87.15.A, 87.17.Jj.

**Keywords:** *Aspergillus Oryzae*, Desolvation, Diffusivities, Nonequilibrium Binding Energy, Translational Entropy, Water

### Graphical Abstract



## 1. Introduction

Over the years, researchers have swept through the discipline of soft matter physics, which aims to clarify how water molecules affect ligand-receptor interaction, binding, stability, *etc.*, in order to effectively create rational drugs. Rational medication design requires a precise treatment of the ligand-host protein interaction <sup>[1]</sup>, which can be improved and directed by knowledge of nonequilibrium binding energy. A thorough grasp of the nonequilibrium binding energy involved in the formation of enzyme-substrate complexes may be useful in understanding other interactions, including those between drugs and proteins, antigens and antibodies, the dreaded SARS-CoV-2 and cell membrane. During the binding relationship between the enzyme and the substrate, which may also be desolvated, it is maintained that water must be displaced from the enzyme's binding sites. According to Szalai *et al.* <sup>[2]</sup>, the binding site water network plays a crucial role in ligand-protein binding, as evidenced by the notable changes in binding enthalpies between light and heavy water. Both the ligand and the protein are solvated before binding in a physiological setting, and at least a partial desolvation of both components occurs throughout the binding process <sup>[2,3]</sup>. When it comes to desolvation and the substitution of ligand-protein and water-water interactions for ligand-water and protein-water interactions, the difference between apolar and polar moieties is essential <sup>[4-7]</sup>.

The thermodynamic stability of the complex formed has always been the main focus of nearly all studies on the role of solvent in ligand-receptor binding. Years ago, the idea of the potential of mean free path, which is similar to Gibbs free energy in relation to complex formation, was of interest. At standard pressure and an appropriate temperature, the potential of mean force, PMF ( $\Delta G(R_0)$ ), depends on the distance ( $R_0$ ) between the two large molecules. The contributions to it come from the entropic ( $-T\Delta S(R_0)$ ) and enthalpic ( $\Delta H(R_0)$ ) terms; the relative percentage of the two contributions depends on  $R_0$ , and the stabilizing effects of the PMF's entropic and enthalpic contributions act in opposite directions to one another <sup>[8]</sup>. This is why the concentration of the reactants (or ligand and receptor) is very relevant. In the logarithmic relationship between  $\Delta G$  and binding affinity ( $K_d$ ), a negative  $\Delta G$  indicates stronger binding or, better yet, greater stability or spontaneity in binding. Water molecules influence enthalpy and entropy, impacting  $\Delta G$  <sup>[9]</sup>. In a study years back, Michel *et al.* <sup>[10]</sup> suggested how removal of water can increase the negative magnitude of the binding free energy change. Accounting for water's influence is crucial when calculating protein-ligand affinity <sup>[11]</sup>. As per  $K_d$ , a dimensionless equilibrium constant had been proposed and used elsewhere <sup>[12,13]</sup> since  $\Delta G/RT$  is dimensionless and there is no basis for a standard state dissociation constant.

In light of the fact that water molecules interact with proteins and ligands during protein-ligand interaction, influencing entropy and enthalpy changes and, ultimately,  $\Delta G$  <sup>[14]</sup>, the question that remains is how many solvents (in this case, water) are likely to be released after the formation of an enzyme-substrate complex. As can be seen from the above, the main focus has been on the importance of the solvent in ligand-receptor binding. Almost no effort is made to measure the quantity of solvent molecules released during the binding contact between the ligand (substrate, pathogen, drug, *etc.*) and the receptor (enzymes, cell membrane,

antibodies, *etc.*) in recent times. The goal of the work was to determine how to calculate the amount of solvent molecules displaced from reactant species using some aspects of bioenergetics principles, since desolvation is a prerequisite for the development of a stable complex. The objectives included figuring out how many molecules of desolvation—that is, how many water molecules are displaced from the receptor-ligand interface during binding interaction—and deriving the appropriate bioenergetics equations that allow them to be achieved.

## 2. Brief Theory

Previously, the motion of dissolved and hydrated particles was described as those that do work over the length of a displacement against viscosity and, in some cases, against opposing attractive or repulsive forces <sup>[15]</sup>. In this brief theory, care is taken to avoid confusing potential and kinetic energies viewed against the backdrop of a scenario of conservative field forces <sup>[16]</sup>. There are two types of forces, namely short- and long-range forces; the latter come into cumulative effect after the long-range forces have narrowed the intermolecular distance. This explains why nonpolar (or hydrophobic) molecules, whether they exist as a homogeneous substance or in combination with other polar substances, have a high melting point. In these situations, bulk and steric factors are not precluded. Moving forward, two equations <sup>[15]</sup> are herein stated as follows:

$$u_i = 4\pi\alpha_E\hat{R}(R_0 - \hat{R})D_E C_{ES} \quad (1)$$

The equation specifies the translational velocity ( $u_i$ ) of any solute in solution up to a target solute where the interparticle distance ( $\hat{R}$ ) is the sum of two radii, namely, the hydrodynamic radii of the substrate, S (or ligand, L), and of the enzyme, E (or receptor, R), designated respectively as  $R_S$  ( $R_L$ ) and  $R_E$  ( $R_R$ ) if there are no perturbative attractive or repulsive forces. In this case the only force originates from the thermal energy of bulk solution.  $D_E$ ,  $C_{ES}$ , and  $R_0$  (to be defined shortly) are the translational diffusion coefficient of E or R if mobile, the molar concentration of ES or RL, representing respectively, the enzyme-substrate complex and receptor-ligand complex if all are mobile, and  $\alpha_E$  and  $\alpha_S$  are given as:

$$\alpha_E = \left(\frac{M_3}{M_2}\right)^{1/2} / [(M_3/M_2)^{1/2} + 1] \quad (2a)$$

$$\alpha_S = \left(\frac{M_2}{M_3}\right)^{1/2} / [(M_2/M_3)^{1/2} + 1] \quad (2b)$$

The alternatives are respectively,  $\alpha_E = 1 - \alpha_S$  and  $\alpha_S = 1 - \alpha_E$ ; each represents a fraction of the total distance covered while advancing towards each other (the enzyme, E, and substrate, S); the lower molar mass solute having a higher fraction than the higher molar mass solute. Of course, this study deals with not less than two species that are mobile in solution. The second equation is:

$$u_i = 4\pi\alpha_S\hat{R}(R_0 - \hat{R})D_S C_{ES} \quad (3)$$

Where the subscript  $S$  refers to the substrate (ligand). Henceforth, the enzyme and substrate will be adopted, and therefore, they may be generalizable to receptors and ligands. If up to a point electrostatic forces come into effect,

the intermolecular distance ( $R_0$ ) where such forces commence needs to be determined. As stated earlier, this section needs to be brief as further details can be found in the literature [15]. The intermolecular distance where attractive or repulsive electrostatic forces commence is given as:

$$R_0 = \frac{\dot{R}}{1 - S_{l-1}/S_{l-2}^2} \tag{4}$$

Where  $S_{l-1}$  is the slope from the plot of the square of the frequency ( $\dot{\nu}$ ) of collision between  $E$  (or  $R$ ) and  $S$  (or  $L$ ) versus  $1/[R_{int} (R_{int} - \dot{R})]$ .  $R_{int}$  is the average intermolecular distance.

Meanwhile, for any two solutes in solution advancing towards each other regardless of any obstacles, if both solutes can be influenced mutually by electrostatic forces (attraction in this case), then there should be two forms of kinetic energy, one of thermal origin and the other of electrostatic origin; hence, Eq. (4) specifies the intermolecular distance at which mutual attractive forces commence. Thus, Newtonian mechanics comes into relevance such that  $mu_2^2 = mu_0^2 + 2F\Delta x$  ( $m$ ,  $u_q$ ,  $u_2$ ,  $\mathcal{F}$ , and  $\Delta x$  are the mass of solute, initial thermally driven velocity, final or peak velocity, force, and distance covered following attractive electrostatic interaction). The electrostatic component creating directionality akin to electrostatic steering [17], earlier shown in the literature [15], is derived in a simpler manner as follows:

$$\phi = 13.8564(\pi\eta R_E P)^{1/2} \epsilon_r \epsilon_0 [R_{int}^3 (R_{int} - \dot{R})] / e^2 \tag{5}$$

$$\dot{\nu} = 0.288675 \left( \frac{P}{\pi\eta R_E R_{int} (R_{int} - \dot{R})} \right)^{1/2} \tag{6}$$

Where  $\dot{\nu}$  is the frequency of collision given by Smoluchowski's equation between the enzyme (the bullet molecule) and the larger molecule, the polysaccharide. The enzyme and the substrate, regardless of size, remain the receptor and ligand, respectively. Smolucowski's equation is  $2\pi\dot{R}D_E C_{ES}$ . Solving for the square root of  $P$  gives:

$$P^{1/2} = \frac{\dot{\nu}[\pi\eta R_E R_{int} (R_{int} - \dot{R})]^{1/2}}{0.288675} \tag{7}$$

Substitute Eq. (7) into Eq. (5) to give:

$$\phi = \frac{\dot{\nu}[13.8564\pi\eta R_E R_{int}^2 (R_{int} - \dot{R})\pi\epsilon_r \epsilon_0]}{0.288675 e^2} \tag{8}$$

Meanwhile, Eqs (5) through (8) are regarded as general equations in that, though  $R_{int}$  represents average intermolecular distance, all equations can have  $R_{int}$  replaced by the intermolecular distance ( $R_0$ ) where electrostatic attraction commences. The physical meaning of  $\phi$  stems from the fact that there are a significant number of cases in which a mixture of solutes comprises small polar, small and large ionic compounds; in all, there could be polar-polar, polar-hydrophobic, ionic-ionic, ionic-polar, and ionic-hydrophobic interactions. Each of them has a descriptive equation, but it is not certain what the net charge of macromolecules like proteins and dipole moment of the polar molecules may be; van der Waals force may not easily be quantifiable on a case-by-case basis. Considering the fact

that there are long- and short-range attractive forces, without information about the net charges and dipole moment, these forces that generate kinetic energy of motion rather than the potential energies (being conventionally negative as the lower values but zero at the highest value by virtue of position relative to another position in space) are summed up to give:

$$2K.E. = \frac{\phi e^2}{4\pi\epsilon_r \epsilon_0 \dot{R}} \tag{9}$$

The sum of all long— and short—range attractive forces, including hydrophobic interactions, may be  $\phi$ —fold greater or less than  $e^2/4\pi\epsilon_r \epsilon_0$ ; if  $\phi > 1$ , it may be greater; if  $\phi < 1$  (a fraction), it may be less. If there are binding interaction between particles with a unit formal charge and weakly polar charge particles,  $\phi < 1$ ; the converse is case if the formal charge is greater than one. The following equations are not meant to be derived but are used to show the difficulty of understanding information about unknown, independent variables, like dipole moments; therefore, they are labeled with separate Roman numbers and used in a qualitative analysis.

$$\beta\omega(R) \approx -\xi_{ii} - \xi_{i-in} - \xi_{in} - \xi_{id} - \xi_{dd} \tag{9i}$$

Where  $(-\xi_{ii})$ ,  $(-\xi_{i-in})$ ,  $(-\xi_{in})$ ,  $(-\xi_{id})$ ,  $(-\xi_{dd})$ ,  $\beta$ , and  $\omega(R)$  are the potential energy of interaction ( $I_E$ ) between two ionic molecules, ion-induced  $I_E$ , induced dipole-dipole (van der Waal's kind)  $I_E$ , ion-dipole  $I_E$ , dipole-dipole  $I_E$ ,  $1/k_B T$  (where  $k_B$  and  $T$  are the Boltzmann constant and thermodynamic temperature respectively), and PMF respectively. As an example of one of those equations is the equation of dipole-dipole  $I_E$  given as [18]:

$$\text{Dipole-dipole interaction energy} = -k_B T \frac{(l_B \mu_A \mu_B)^2}{3R^6} \tag{9ii}$$

Where  $R$ ,  $l_B$ , and  $\mu$  are the distance between interacting particles, Bjerrum length, electric dipole moment respectively. Regarding the  $I_E$  for strongly ionized protein—polysaccharide with a net charge in the protein while the polysaccharide is polar, in a given buffer, the  $\omega(R)$  [15] is given as:

$$V_{2-3S} = \frac{-(l_B Z_2 \mu_S)^2 (e^{-\kappa(R-a)})^2}{6R^4 (1+\kappa a)^2} \tag{9iii}$$

$\kappa$  and  $a$  are the inverse Debye screening length and the closest distance between the “central ion” (protein b or any other charged substrate such as phosphate containing starch) and surrounding ions which is approximately the protein radius respectively. The overall kinetic energy, a summation of long range and all available short range energies is given as:

$$\frac{\phi e^2}{8\pi\epsilon_r \epsilon_0} = -\beta\omega(R)/2 \tag{9iv}$$

To some degree of specifics, one may have:

$$\frac{\phi e^2}{8\pi\epsilon_r \epsilon_0} = -k_B T \frac{(l_B \mu_A \mu_B)^2}{3R^6} - \frac{(l_B Z_2 \mu_S)^2 (e^{-\kappa(R-a)})^2}{6R^4 (1+\kappa a)^2} - \dots \tag{10}$$

Given that achieving near-accuracy in all measurements is a daunting task, the first part of the qualitative analysis involves figuring out how to locate all independent variables and, maybe, every type of operational  $I_E$  by exploring very complex instrumentation. Structural analysis of the large molecules and the complex formed are not avoidable. A way out is the formulation of a sort of quasi-Coulomb equation on account of which the factor  $\phi$ ,  $\phi$ , has to be substituted into Eq. (10). Next substitute Eq. (8) in which  $R_{int}$  is substituted for  $R_0$  into Eq. (9) to give:

$$\xi_{El} = \frac{\psi[12\pi\eta R_E R_0^2 (R_0 - \hat{R})]}{\hat{R}} \quad (11)$$

The total energy ( $\xi_{TI}$ ), combining thermal and electrostatic energies for the two particles moving towards each other, is given as:

$$\begin{aligned} \xi_{TI} &= 6\pi\eta R_E * 4\pi\epsilon_0 \hat{R} (R_0 - \hat{R})^2 D_E C_{ES} + 6\pi\eta R_S * 4\pi\epsilon_0 \hat{R} (R_0 - \hat{R})^2 D_S C_{ES} + \frac{\psi[24\pi\eta R_E R_0^2 (R_0 - \hat{R})]}{2\hat{R}} + \frac{\psi[24\pi\eta R_S R_0^2 (R_0 - \hat{R})]}{2\hat{R}} \\ &= 24\pi\eta \left[ R_E \epsilon_0 (\pi \hat{R} (R_0 - \hat{R})^2 D_E C_{ES} + \frac{R_0^2 (R_0 - \hat{R}) \psi}{2\hat{R}}) + R_S \epsilon_0 (\pi \hat{R} (R_0 - \hat{R})^2 D_S C_{ES} + \frac{R_0^2 (R_0 - \hat{R}) \psi}{2\hat{R}}) \right] \quad (12) \end{aligned}$$

Note that the substitution of Eqs (1) and (2) separately into  $6\pi\eta R_E$  and  $6\pi\eta R_S$  respectively and multiplying respectively by  $\epsilon_0 (R_0 - \hat{R})$  and  $\epsilon_0 (R_0 - \hat{R})$  give the work done against the resistance of the medium. Meanwhile,  $\xi_{TI}$  is equal to the sum of all thermal energies ( $\xi_{ST}$ ) driving the motion of the solution components, including some (if not all) of the departing water of hydration. Going forward, the reader is reminded that the effective energy ( $\xi_{eff}$ ) of motion in a given liquid solvent or mixture in a liquid state, under the influence of thermal energy, is given as [19]:

$$\xi_{eff} = \left[ m_i \left( \frac{6k_B T D_i}{L} \right)^2 \right]^{1/3} \quad (13)$$

Where,  $L$ ,  $k_B$ ,  $T$ ,  $m_i$  and  $D_i$  are respectively, the cube root of the molar volume of the solvent (water), Boltzmann constant, thermodynamic temperature, mass of any solution component, and translational diffusion coefficient of solution components. Expectedly high-ranking scholars, notably in advanced scientific communities in the Americas, Europe, and Asia, etc., may raise objections, but it is inconceivable that biological fluid components, such as water, can possess thermal energy equal to  $3 k_B T$  as to imply “a reverse unguided evolution” akin to “an American and in particular Indian action movie in which the lead actor disappears into the thin air from the roof of a high-rise building; of course, the movie producers advise the young ones against any attempt to replicate such action.”

$$\xi_{ST} = \left[ m_S \left( \frac{6k_B T D_S}{L} \right)^2 \right]^{1/3} + \left[ m_E \left( \frac{6k_B T D_E}{L} \right)^2 \right]^{1/3} + \Phi_d \left[ m_W \left( \frac{6k_B T D_W}{L} \right)^2 \right]^{1/3} \quad (14)$$

Where  $m_W$  and ‘ $\Phi_d$ ’ are respectively, the mass of one molecule of water and number of water molecules released per enzyme-substrate (ES) complex formation.

$$\xi_{ST} = \left( \frac{36k_B^2 T^2}{L^2} \right)^{1/3} (D_S^{2/3} m_S^{1/3} + D_E^{2/3} m_E^{1/3} + \Phi_d D_W^{2/3} m_W^{1/3}) \quad (15)$$

Given that  $\xi_{ST} = \xi_{TI}$  (Eq. (12)), then, for the purpose of simplicity, consider the following:

$$\bar{\epsilon} = R_E \epsilon_0 \left( \pi \hat{R} (R_0 - \hat{R})^2 D_E C_{ES} + \frac{R_0^2 (R_0 - \hat{R}) \psi}{2\hat{R}} \right)$$

$$\hat{\epsilon} = R_S \epsilon_0 \left( \pi \hat{R} (R_0 - \hat{R})^2 D_S C_{ES} + \frac{R_0^2 (R_0 - \hat{R}) \psi}{2\hat{R}} \right)$$

$$\Phi_d = \frac{1}{D_W^{2/3} m_W^{1/3}} \left[ 24\pi\eta \left( \frac{L^2}{36k_B^2 T^2} \right)^{1/3} (\bar{\epsilon} + \hat{\epsilon}) - (D_S^{2/3} m_S^{1/3} + D_E^{2/3} m_E^{1/3}) \right] \quad (16)$$

### 3. Materials and Methods

#### 3.1 Equipment

An electronic weighing machine was purchased from Wensler Weighing Scale Limited, and a 721/722 visible spectrophotometer was purchased from Spectrum Instruments, China. A hand pH meter was purchased from Hanna Instruments, Italy.

#### 3.2 Chemicals and their preparation

As explored in earlier studies [20], *Aspergillus oryzae* alpha-amylase (EC 3.2.1.1) and insoluble potato starch, whose molar mass is  $\sim 64540$  kg/mol [21] were purchased from Sigma-Aldrich, USA. Tris HCL, 3, 5-dinitrosalicylic acid, maltose, and sodium potassium tartrate tetrahydrate were purchased from Kem Light Laboratories in Mumbai, India. Hydrochloric acid, sodium hydroxide, and sodium chloride were purchased from BDH Chemical Ltd., Poole, England. Distilled water was purchased from the local market. The molar mass of the enzyme is 52 k Da [22]. A gelatinized insoluble potato starch whose concentration is equal to 1 g/100 mL was subjected to serial dilution give concentrations ranging between 5 and 10 g/L for the assay in which  $[S_0] \gg [E_0]$  (0.0005 g/L). A concentration of *A. oryzae* alpha-amylase equal to 0.0005 g/L was prepared in a Tris HCl buffer solution at a pH of 7.0.

#### 3.3 Method

The enzyme was assayed using gelatinized potato starch in accordance with Bernfeld's (3, 5-dinitrosalicylic acid) technique [23]. Using maltose as a standard, the amount of reducing sugar generated after the substrate hydrolyzed in three minutes was measured at 540 nm, with an extinction coefficient of 181 L/mol.cm. The assay was carried out at 25°C. The maximum intermolecular distance ( $R_{int}$ ) was determined using the equation:  $R_{int} = (V/(n_E + n_S)N_A)^{1/3}$  where  $n_E$ ,  $n_S$ ,  $V$ , and  $N_A$  are number of moles of the enzyme and substrate, volume of the reaction mixture, and Avogadro's number respectively. The minimum intermolecular distance wherein mutual electrostatic perturbation commences is determined as described elsewhere [15]. The diffusion coefficient of the starch was computed using the equation for large molar mass polymers given as  $D_2 = D_1 (M_1/M_2)^{1/3}$  where  $M_2 > M_1$ ; the latter represent different molar masses while the  $D_s$  are different diffusivities ( $D_1 > D_2$ ). The hydrodynamic radius of the starch computed using Stokes-Einstein equation is that of a sphere whose volume is equal to that of a nonspherical starch polymer. The diffusivity of water at 298.15 K used was 2.3  $exp. (-11) m^2/s$  [24]. That of *A. oryzae* was computed using an arbitrarily chosen radius of 2.51 nm substituted into Stokes-Einstein equation.

#### 3.4 Statistics

The mean catalytic velocity of hydrolysis of gelatinized starch was calculated using a Casio scientific calculator (fx-

991MS-China). Gaussian statistics are not appropriate. Thus, the best method for determining the variance ( $\sigma^2$ ) and, in turn, the standard deviation for a population ( $n$ ) of size three is to use a nonparametric statistical approach [25]. Results are presented as mean  $\pm$  SEM. Hozo *et al.* [25] equation is:

$$\sigma^2 = \frac{(n+1)[(n^2+3)(a-2m+b)^2+4n^2(b-a)^2]}{48n(n-1)^2} \quad (17)$$

Where  $n$ ,  $a$ ,  $b$ , and  $m$  are the size of the sample (data points, 3 in this research), the smallest value, the largest value, and the median respectively. Microsoft Excel (2010) was used to carry out graphical plots.

#### 4. Results and Discussion

##### 4.1 Results

Moving forward, the number of molecules of the enzyme-substrate (ES) complex is computed as shown in Table 1. Such parameter is used for the computation of the frequency of collision between the enzyme and the substrate using Smolucowski's equation. The frequency is needed for the graphical determination of the first and second slopes stated in Eq. (4).

**Table 1:** The velocities ( $v$ ) of hydrolysis of gelatinized starch and the number ( $N_{ES}$ ) of molecules of ES complex

[S <sub>0</sub> ]/g/l	$v/exp. (-5) /mol./l/min$	$N_{ES} / exp. (+18)$
5	6.493±0.118	3.72±0.035
6	6.852±0.052	3.90±0.023
7	7.324±0.106	4.12±0.023
8	7.452±0.091	4.27±0.023
9	7.657±0.175	4.39±0.021
10	7.847±0.101	4.50±0.018

Molar concentrations were adopted for computational convenience.

The computed  $R_{int}$  values are used for the computation of the minimum intermolecular distance,  $R_0$  and the differences between them and the sum of the hydrodynamic radii of the substrate and enzyme as shown in Table 2; the computation of  $R_0$ , requires that the slopes indicated in Eq. (4) have to be graphically determined. The first slope is derived from Fig 1.

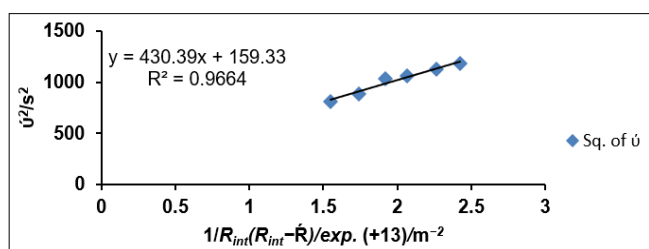


**Fig 1:** Determination of the first slope  $S_{l-1} = 430.39 \text{ exp. } (-13) \text{ m}^2/\text{s}^2$

The second slope is derived from Fig 2.

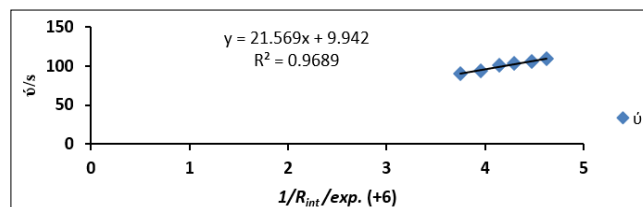


**Fig 2:** Determination of the second slope  $S_{l-2} = 21.569 \text{ exp. } (-6) \text{ m/s}$

**Table 2:** Intermolecular distance ( $R_{int}$ ) and difference between  $R_{int}$  and sum of hydrodynamic radii ( $\bar{R}$ ) of two different molecules

$R_{int}/exp. (-7)/m$	2.671	2.530	2.414	2.331	2.233	2.161
$(R_{int}-\bar{R})/exp. (-7)/m$	2.416	2.275	2.159	2.073	1.979	1.906

The first slope ( $S_{l-1}$ ) for the computation of intermolecular distance ( $R_0$ ) where longer range electrostatic attraction began is obtained from the plot of  $v^2$  versus  $1/R_{int} (R_{int}-\bar{R})$ ; the second slope ( $S_{l-2}$ ) is obtained from the plot of  $v$  versus  $1/R_{int}$ . [15]. Eq. (4) is fitted to the two slopes for the computation of  $R_0$  (40.436 nm);  $R_0-\bar{R} = 3.74089$  nm;  $\bar{R} = R_E + R_S = 36.6953$  nm;  $R_S = 34.18532358$  nm

All the relevant values in Tables 1 and 2 were deployed and substituted into the relevant equations in the theoretical section to give for the first time, number of water of desolvation. Expectedly, the number of water of desolvation showed increasing trend with increasing substrate concentration (Table 3). The cognate entropy changes, which also showed a similar trend, were computed based on the assumption that there is an increase in the number of free solvent molecules in the bulk following desolvation, which translates into an increase in entropy in a reaction volume of one cubic meter. The values of the water of desolvation,  $\Phi_d$  per ES, ranged between approximately 338 and 400, while the total,  $\Phi_d * N_{ES}$ , ranged between 1.3 and 1.85 *exp. (+21)*; the cognate entropic energy, the translational entropy change, ranged between 93.06 and 136.70 *exp. (-3) J/mol K*. As stated in the footnote of Table 3, the maximum amount of water of desolvation and, hence, the entropic term were calculated based on the idea that the water of desolvation can be thought of as a product in a reaction mixture that complies with Michaelian kinetics. At saturation level ( $[ES]=[E_0]$ ), the maximum  $\Phi_d$ ,  $\Phi_d * N_{ES}$ , and  $T\Delta S_{trans}$  values were 526.316, 3.048 *exp. (+21)*, and 216.129 *exp. (-3) J/mol. K*, respectively.

**Table 3:** Number ( $\Phi_d$ ) of water molecules per ES, total displaced and translational entropy ( $\Delta S_{trans}$ ) gain of displaced water molecules

[S <sub>0</sub> ]/g/L	5	6	7	8	9	10
$\Phi_d$	337.68	358.34	382.28	391.66	391.66	399.79
$\Phi_d * N_{ES} (exp. (+21))$	1.256	1.398	1.606	1.672	1.755	1.845
$T\Delta S_{trans} / exp. (-3) (J/mol. K)$	93.06	103.58	118.99	123.88	130.03	136.70

Maximum  $\Phi_d$ ,  $\Phi_d * N_{ES}$ , and  $T\Delta S_{trans}$  values at saturation level ( $[ES]=[E_0]$ ) were 526.316, 3.048 *exp. (+21)*, and 216.129 J/mol. K *exp. (-3)* respectively. The translational entropy of the departing water molecules in the course of desolvation is computed under the premise that there is an increase in the number of free solvent molecules in the bulk, which translates into an increase in entropy in a reaction volume of one cubic meter. Thus, entropic energy is given as:  $T\Delta S_{trans} = RT \ln \frac{18(\Phi_d N_{ES} \times exp. (-3) + N_A/18)}{N_A}$  where  $R$  is the universal gas constant.

## 4.2 Discussion

This discussion serves to relate water of desolvation and translational entropy in this study to literature concern for the binding process enhanced by desolvation. The argument that the decrease in water-accessible surface area upon folding leads to a significant increase in water's translational entropy, overcoming the loss of protein's conformational entropy [26], may also explain the driving force behind ligand-receptor (LR which could be ES) complex formation. The entropic gain, driven by water molecules' freedom of movement, may be a key factor in stabilizing the folded protein structure besides the impact of hydrogen bond networks. This suggestion, however, is of hypothetical significance. Nonetheless it may be relevant in the stability of LR. Examples of concern for the release of water in the course of binding had been for decades as stated earlier. Thus, there is the case of hinge motions involving the ATP lid domain and the nucleoside monophosphate binding domain closing over their respective substrates, in which water is excluded from the enzyme's active site during the phosphoryl transfer reaction [27, 28]. In other scenarios the source of an entropy increase following the binding of a ligand to a receptor, is the release of the water molecules from the binding pocket and from around the ligand to get more freedom in the bulk phase, purported to be investigated with unspecified, newly developed method [29]. It is equally expedient to realize that desolvation is not total, particularly with respect to the enzyme, which requires conserved water for catalysis and stability. This notwithstanding, there are inner and outer hydration layers in which there are grades of water densities; some have greater electrostriction than the others. The idea that "prior to binding, the ligand-free binding pocket is occupied by water molecules characterized by a paucity of H-bonds and high mobility resulting in an imperfect hydration of the critical residue Asp189" [30] of the enzyme supports the problem of loosely bound water molecules, which are likely to easily undergo desolvation. For instance, crucial residue Asp189 of the lipase active site is not fully hydrated because water molecules with a high degree of mobility (loosely bound water molecules) and few H-bonds occupy the ligand-free binding pocket before binding. This phenomenon can enhance the elucidation of how water affects protein-ligand recognition and is probably a major factor driving ligand binding via water displacement [30]. Further to this, is the observed decrease in protein dynamics consistent with the measured decrease in the intrinsic volume,  $V_M$  (1.4–2.1%), of RNase A upon the binding to 2'-CMP or 3'-CMP [31]. This information, applicable to any other enzyme-substrate binding reaction, such as the one with gelatinized starch and amylase in this study, suggests that the binding of 2'-CMP or 3'-CMP to RNase A releases between  $210 \pm 40$  water molecules to the bulk state [31]. This value (210), though not within the range of 338 to 400 (Table 3) reported in this study for amylase, is nevertheless good evidence that the model developed in this study could be valid.

The reaction rate can change in response to the amount of water content in a reaction mixture. Desolvation is likely a type of enzyme or substrate dependence that varies among different enzymes. Studies on *Candida rugosa* lipase using different liquids as medium of reaction, showed that the highest reaction rate was obtained in n-hexane and the ionic

liquid [BMIM]PF<sub>6</sub> when the concentrations of water were 0.15 mol/dm<sup>3</sup> and 0.38 mol/dm<sup>3</sup>, respectively. In the more polar tetrahydrofuran, [BMIM]BF<sub>4</sub> esters were produced at a very low reaction rate which was observed to be only slightly dependent on the concentration of water [32]. The number of water molecules released could dependent on the composition of reaction medium, pH, temperature, ionic strength, nature of the substrate and enzyme. Furthermore, a high concentration of the enzyme or substrate results in high viscosity, low water potential, and reduced translational velocities, which reduce the likelihood that there are enough water molecules in the outer hydration layer to be displaced and, in turn, lower the velocity of product formation.

The solvation free energy change is attributed to the solvation structure change due to the ligand binding by the host protein [1]. The solvation structure is changed when the ligand binds to its recognition site because the hydrogen bonds are broken, rearranging the hydrogen bond network in the solvent water. Understanding the thermodynamic process of molecule recognition is essential since this change in solvation also modifies the solvent's entropy [1]. In particular, it has been proposed that the expulsion of thermodynamically unfavorable water molecules during complex formation enhances the ligand's affinity [33, 34]. This may be in line with the finding in this study that the translational entropy gain ranging between 93.06 and 136.70 *exp.* (–3) J/mol K of the departing water molecules (desolvation) enhances and stabilizes the complex. Additionally, it should be noted that not only the protein but also the ligand itself needs to be, at least partially, desolvated and thereby influence binding. Research has shown that hydrogen bonds can enhance binding when both the donor and acceptor have significantly stronger or weaker hydrogen bonding capabilities than water, while mixed strong-weak pairings can decrease affinity due to interference with bulk water [14].

Based on all related issues in the literature, one can state in summary that water displacement typically contributes to favorable entropy ( $T\Delta S > 0$ ) and enthalpy ( $\Delta H < 0$ ) changes, which, when combined with hydrogen bonding changes that affect  $\Delta H$  either positively or negatively, will ultimately affect the overall  $\Delta G$  [35]; if stronger hydrogen bonds are formed between the protein and ligand,  $\Delta H$  decreases, stabilizing the complex; however, if hydrogen bonds are broken without equivalent replacements, the enthalpy may increase, making the binding less favorable [35]. Thus, it appears that low water potential bulk concentration and insufficient solvent desolvation may inhibit the formation of the LR complex. A minimum water potential is necessary for the complex's functional groups and the loose outer hydration layer to form a network of hydrogen bonds, as well as for translational motion that can bring the enzyme and substrate close together.

## 5. Conclusion

The derived equations could be deployed for the computation of the water of desolvation following ligand-receptor binding, exemplified by the results from this study, which showed a range of 338 to 400 water molecules per molecule of complex with a corresponding thermodynamic component, translational entropy gain ranging between 93.06 and 136.70 *exp.* (–3) J/mol K. Further thermodynamic

characterization of ligand-receptor binding on the basis of desolvation needs to be done at different temperatures in the future. That will entail the use of nonequilibrium binding energy to generate a number of waters of desolvation at different temperatures, which, as long as such water molecules are regarded as by products, could be fitted to the Michaelian equation, as was done in this research.

#### 6. Disclaimer (Artificial intelligence)

Author(s) hereby declare that NO generative AI technologies such as Large Language Models (ChatGPT, COPILOT, etc.) and text-to-image generators have been used during the writing or editing of this manuscript.

#### 7. Disclaimer

The preprint document is available in these links:

viXra:2506.00

<https://hal.science/hal-05117586v1>

<https://dx.doi.org/10.2139/ssrn.5323475>

#### 8. Dedication

Dr. (Honoris Causa) Samuel Osaigbovo Ogbomudia (Brigadier General) was one-time military governor of the defunct Mid-West State of Nigeria and in the latter years became an active politician. Among many selfless accomplishments, only one is intentionally mentioned. This is the establishment of the state transport company. The vehicles were not customized after his name; rather, they were given the inscription "Mid-West Line," which greatly influenced private investors within and out of the state to establish transport companies in which their vehicles bore the inscription, the name, and then "Line," e.g., "Ekenedilichukwu Line." The state transport company was efficient and profitable. To him, I dedicate this study for his selfless service to humanity.

#### 9. Acknowledgement

I am very grateful to my siblings for their financial and in-kind support. Grammar-checking services by QuillBot Company are also appreciated.

#### 10. Authors' contributions

The sole author designed, analyzed, interpreted and prepared the manuscript.

#### 11. Consent

NA.

#### 12. Ethical approval (where ever applicable)

NA.

#### 13. References

1. Yoshida N. Role of solvation in drug design as revealed by the statistical mechanics integral equation theory of liquids. *J. Chem. Inf. Model.* 2017; 57(11):2646-2656. Doi: 10.1021/acs.jcim.7b00389
2. Szalai TV, Bajusz D, Börzsei R, Zsidó BZ, Ilaš J, Ferenczy GG, *et al.* Effect of water networks on ligand binding: Computational predictions *vs* experiments. *J Chem Inf Model.* 2024; 64(23):8980-8998. Doi: 10.1021/acs.jcim.4c01291
3. Fan Z, Zhang J, Wu L, Yu H, Li J, Li K, *et al.* Solvation structure dependent ion transport and desolvation mechanism for fast-charging Li-ion batteries. *Chem. Sci.* 2024; 15:17161-17172. Doi: 10.1039/d4sc05464d
4. Steve W, Homans SW. Water, water everywhere - except where it matters? *Drug Discov Today.* 2007; 12(13-14):534-539. Doi: 10.1016/j.drudis.2007.05.004
5. Ferency GG, Keseru GM. Thermodynamics of fragment binding. *J. Chem. Inf. Model.* 2012; 52(4):1039-1045. Doi: 10.1021/ci200608b
6. Giordanetto F, Jin C, Willmore L, Feher M, Shaw DE. Fragment hits: What do they look like and how do they bind? *J. Med. Chem.* 2019; 62:3381-3394. Doi: 10.1021/acs.jmedchem.8b01855
7. Maurer M, Oostenbrink C. Water in protein hydration and ligand recognition. *J Mol Recognit.* 2019; 32:e2810. Doi: 10.1002/jmr.2810
8. Choudhury N, Pettitt BM. Enthalpy-entropy contributions to the potential of mean force of nanoscopic hydrophobic solutes. *J Phys Chem B.* 2006; 110(16):8459-8463. Doi: 10.1021/jp056909r
9. Qu X, Dong L, Luo D, Si Y, Wang B. Water network-augmented two-state model for protein-ligand binding affinity prediction. *J. Chem. Inf. Model.* 2024; 64(7):2263-2274. Doi: 10.1021/acs.jcim.3c00567
10. Michel J, Tirado-Rives J, Jorgensen WL. Energetics of displacing water molecules from protein binding sites: Consequences for ligand optimization. *J. Am. Chem. Soc.* 2009; 131(42):15403-15411. Doi: 10.1021/ja906058w
11. Zsidó BZ, Hetényi C. The role of water in ligand binding. *Curr. Opin. Struct. Biol.* 2021; 67:1-8. Doi: 10.1016/j.sbi.2020.08.002
12. Udemá II, Onigbinde AO. Enzymatic kinetic issues and controversies surrounding Gibbs free energy of activation and Arrhenius activation energy. *Asian J Phys Chem Sci.* 2019; 7(4):1-3 Doi: 10.9734/AJOPACS/2019/v7i430103
13. Udemá II. In A Pathophysiologic state due to SARS-CoV-2, viscosity and cholesterol are double-edged swords. *Int. J. Pathog. Res.* 2025; 14(3):81-99. Doi: 10.9734/ijpr/2025/v14i3365
14. Chen S, Wang Z-G. Using implicit-solvent potentials to extract water contributions to enthalpy-entropy compensation in biomolecular associations. *J. Phys. Chem. B.* 2023; 127:6825-6832. Doi: 10.1021/acs.jpcc.3c03799
15. Udemá II. The key to effective catalytic action is pre-catalytic site activity preceding enzyme-substrate complex formation. *Adv Res.* 2017; 9(3):1-12. Doi: 10.9734/AIR/2017/32676
16. Udemá II. Effect of salts and organic osmolytes is due to conservative forces. *Asian J. Appl. Chem. Res.* 2020; 5(1):1-17. Doi: 10.9734/AJACR/2020/v5i130123
17. Wade RC, Gabdoulina RR, Lüdemann SK, Lounnas V. Electrostatic steering and ionic tethering in enzyme-ligand binding: Insights from simulations. *Proc. Nat. Acad. Sci. U.S.A.* 1998; 95(11):5942-5949. Doi: 10.1073/pnas.95.11.5942
18. Lund M. Electrostatic interactions in and between biomolecules Lund University Ph.D. Thesis, 2006.
19. Udemá II. Determination of translational velocity of reaction mixture components: Effect on the rate of reaction. *Adv. Biochem.* 2016; 4(6):84-93. Doi: 10.11648/j.ab.20160406.13

20. Udema II. Directly and indirectly determinable rate constants in Michaelian enzyme-catalyzed reactions. *Asian J. Biochem. Genetics Mol Biol.* 2023; 15(1):41-55. Doi: 10.9734/AJBGMB/2023/v15i1327
21. Tomasik P. Specific chemical and physical properties of potato starch. *Food.* 2009; 9:45-46.
22. Sugahara M, Takehira M, Yutani K. Effect of heavy atoms on the thermal stability of  $\alpha$ -amylase from *Aspergillus oryzae*. *PloS One.* 2013; 8(2):e57432. Doi: 10.1371/journal.pone.0057432
23. Bernfeld P. Amylases, alpha and beta, *Methods. Enzymol.* 1955; 1:149-152. Doi: 10.1016/0076-6879(55)01021-5
24. Camposano AVC, Nordhagen EM, Sveinsson HA, Malthe-So Rensen A. Genetic algorithm workflow for parameterization of a water model using the vashishta force field. *J. Phys. Chem. B.* 2025; 129(4):1331-1342. Doi: 10.1021/acs.jpcc.4c06389
25. Hozo SP, Djulbegovic B, Hozo I. Estimating the means and variance from the median range and the size of a sample. *BMC Med. Res. Methodol.* 2005; 5(13):1-10. Doi: 10.1186/1471-2288-5-13
26. Harano Y, Kinoshita M. Translational-entropy gain of solvent upon protein folding. *Biophys. J.* 2005; 89(4):2701-2710. Doi: 10.1529/biophysj.104.057604
27. Vonrhein C, Schlauderer GJ, Schulz GE. Movie of the structural changes during a catalytic cycle of nucleoside monophosphate kinases. *Structure (London, England: 1993).* 1995; 3(5):483-490.
28. Müller CW, Schlauderer GJ, Reinstein J, Schulz GE. Adenylate kinase motions during catalysis: An energetic counterweight balancing substrate binding. *Structure (London, England: 1993).* 1996; 4(2):147-156. Doi: 10.1016/s0969-2126(96)00018-4
29. Ahmad M, Kalinina O, Lengauer T. Entropy gain due to water release upon ligand binding. *J. Cheminform.* 2014; 6(Suppl 1):35. Doi: 10.1186/1758-2946-6-S1-P35
30. Schiebel J, Gaspari R, Wulsdorf T, Ngo K, Sohn C, Schrader TE, *et al.* Intriguing role of water in protein-ligand binding studied by neutron crystallography on trypsin complexes. *Nat. Commun.* 2018; 9(1):3559. Doi: 1038/s41467-018-05769-2
31. Dubins DN, Filfil R, Macgregor RB, Chalikian TV. Role of water in protein-ligand interactions: Volumetric characterization of the binding of 2'-CMP and 3'-CMP to ribonuclease. *A J. Phys. Chem. B.* 2000; 104(2):390-401. Doi: 10.1021/jp992138d
32. Lajtai-Szabó P, Nemestóthy N, Gubicza L. The role of water activity in terms of enzyme activity and enantioselectivity during enzymatic esterification in nonconventional media. *Hung. J. Ind. Chem.* 2020; 48(2):9-12. Doi: 10.33927/hjic-2020-22
33. Young T, Abel R, Kim B, Berne BJ, Friesner RA. Motifs for molecular recognition exploiting hydrophobic enclosure in protein-ligand binding. *Proc. Nat. Acad. Sci. U.S.A.* 2007; 104(3):808-813. Doi: 10.1073/pnas.0610202104
34. Abel R, Salam NK, Shelley J, Farid R, Friesner RA, Sherman W. Contribution of explicit solvent effects to the binding affinity of small-molecule inhibitors in blood coagulation factor serine proteases. *Chem Med Chem.* 2011; 6(6):1049-1066. Doi: 10.1002/cmdc.201000533
35. Zhang D, Meng Q, Guo F. Incorporating water molecules into highly accurate binding affinity prediction for proteins and ligands. *Int J Mol Sci.* 2024; 25(23):12676. Doi: 10.3390/ijms252312676